© 2019. Published by The Company of Biologists Ltd | Development (2019) 146, dev166017. doi:10.1242/dev.166017

STEM CELLS AND REGENERATION

RESEARCH ARTICLE

BMP signaling is required for amphioxus tail regeneration

Yujun Liang[1,*], Delima Rathnayake[1], Shibo Huang[1], Anjalika Pathirana[1], Qiyu Xu[1] and Shicui Zhang[1,2,*]

ABSTRACT

Amphioxus, a cephalochordate, is an ideal animal in which to address questions about the evolution of regenerative ability and the mechanisms behind the invertebrate to vertebrate transition in chordates. However, the cellular and molecular basis of tail regeneration in amphioxus remains largely ill-defined. We confirmed that the tail regeneration of amphioxus *Branchiostoma japonicum* is a vertebrate-like epimorphosis process. We performed transcriptome analysis of tail regenerates, which provided many clues for exploring the mechanism of tail regeneration. Importantly, we showed that BMP2/4 and its related signaling pathway components are essential for the process of tail regeneration, revealing an evolutionarily conserved genetic regulatory system involved in regeneration in many metazoans. We serendipitously discovered that *bmp2/4* expression is immediately inducible by general wounds and that expression of *bmp2/4* can be regarded as a biomarker of wounds in amphioxus. Collectively, our results provide a framework for understanding the evolution and diversity of cellular and molecular events of tail regeneration in vertebrates.

KEY WORDS: Tail regeneration, Amphioxus, Transcriptome, BMP signaling

INTRODUCTION

Regeneration is the ability to reproduce a missing part of the body, which is widely observed in metazoans. In general, there are two modes of regeneration: (1) morphallaxis, which involves a dramatic re-deployment of existing cells in the absence of active cell proliferation, and (2) epimorphosis, which involves cell proliferation and the formation of a typical blastema (Tanaka and Reddien, 2011; Li et al., 2015). It is clear that regeneration varies substantially from invertebrates to vertebrates (Dinsmore, 1991; Li et al., 2015). Some animals, such as hydra, planaria and starfish, show a remarkable ability to regenerate and are capable of regenerating an entire individual from a small body fragment, whereas other animals, such as birds, nematodes and leeches, have largely or completely lost the ability to regenerate (Bely and Nyberg, 2010; Goss, 1969; Vorontsova and Liosner, 1960). Regeneration can vary even among the parts of the same organism. For instance, many annelid worms can regenerate a tail but not a head (Bely, 2006). Uncovering the molecular mechanisms of regeneration and their evolutionary variations is one of the most important challenges in modern biology. However, our knowledge of this is rather limited and incomplete to date.

[1]Department of Marine Biology, Institute of Evolution and Marine Biodiversity and College of Marine Life Science, Ocean University of China, Qingdao 266003, China. [2]Laboratory for Marine Biology and Biotechnology, Qingdao National Laboratory for Marine Science and Technology, Qingdao 266003, China.

*Authors for correspondence (liangyujun@ouc.edu.cn; sczhang@ouc.edu.cn)

Y.L., 0000-0002-1253-8364; D.R., 0000-0003-4953-441X; S.H., 0000-0001-8426-1846; A.P., 0000-0002-7177-9942; Q.X., 0000-0002-0714-5814; S.Z., 0000-0002-7488-6487

Received 27 March 2018; Accepted 17 January 2019

Amphioxus, a cephalochordate, is the most basal living chordate, and has many anatomical, developmental and genomic similarities to vertebrates. Thus, it is an ideal animal in which to investigate the evolution of regenerative ability and mechanisms in chordates from the invertebrate to vertebrate transition. In fact, amphioxus has long been used to study regeneration, and the history of studies on regeneration of amphioxus has been recently reviewed (Somorjai, 2017). It was initially reported to possess a generally poor potential to replace lost body parts (Biberhofer, 1906; Probst, 1930) but was later shown to have a remarkably high capacity to regenerate tail and oral cirri after amputation (Somorjai et al., 2012a; Kaneto and Wada, 2011; Silva et al., 1998). Recently, it has been shown that the activation of satellite-like Pax3/7 progenitor cells, Wnt signaling and *msx* are linked to tail regeneration in amphioxus (Somorjai et al., 2012a,b). In addition, the neural differentiation marker *soxB2* is expressed in the regenerating ependymal tube (Somorjai et al., 2012a). However, the cellular and molecular basis of tail regeneration in amphioxus is still not well defined. Therefore, the present study focused on exploring the answers to these questions.

RESULTS

The regeneration of amphioxus is a vertebrate-like epimorphic process

Pilot experiments showed that 75 out of 100 amphioxus with a body length less than 1.5 cm (1 year old) survived and formed a blastema at 5-7 days after tail amputation; 93 out of 100 amphioxus with a body length ranging from 2.5 to 3.3 cm (2 years old) survived and formed a blastema at 12-15 days after tail amputation; and all 100 amphioxus with a body length greater than 4 cm (more than 3 years old) survived, but only 54 animals formed a blastema at 20 days after tail amputation. This result was in accordance with the general notion, observed in other regenerative species, that young animals tend to possess a stronger capacity for regeneration than do old ones. To avoid the experimental discrepancy caused by different animal sizes, we thus selected animals with a body length of approximately 3 cm for this study.

To detail the tail regeneration process, both morphological observation and histological analysis were performed during the regeneration process. After amputation, the injury went through a complex period of changes in the pre-existing tissues and the healing process was slightly different from that of European amphioxus *Branchiostoma lanceolatum* and that of the limb regeneration of the urodele. In adult amphioxus *B. lanceolatum*, it takes approximately 1-2 days to fulfill this process (Somorjai, et al., 2012a). In the adult newt, immediately after amputation, the epidermal cells from the circumference of the stump migrate to cover the wound site, and this wound-healing phase is complete within 24 h (Repesh and Oberpriller, 1978). In contrast, in amphioxus *B. japonicum*, the wound surface was not completely covered by the epithelial cell layer until 10 days after amputation (Fig. 1A-C,I,J). At 12-15 days, the blastema protruded with a smooth outer contour, which consisted of cells such as mesenchymal cells (Fig. 1D,K). With growth of the blastema in the following days, newly formed tissues, such as the

Development (2019) 146, dev166017. doi:10.1242/dev.166017

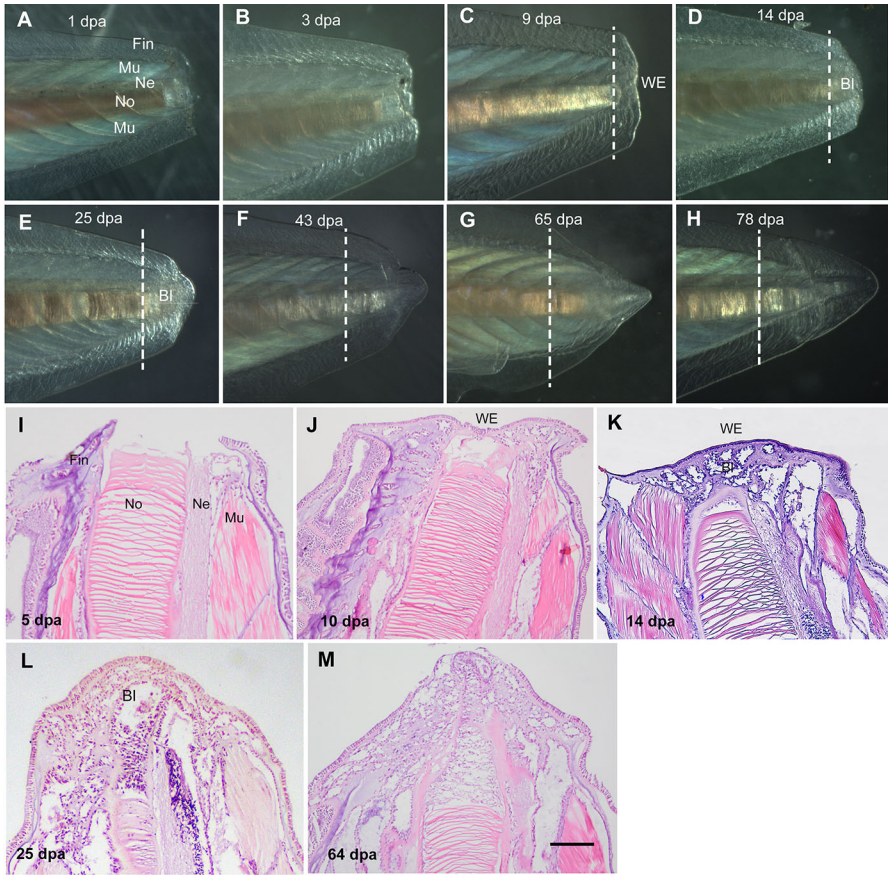

Fig. 1. Tail regeneration process in amphioxus. (A-H) Morphological observations of the tail regeneration process from 1 to 78 dpa. (I-M) Hematoxylin and Eosin staining of longitudinal sections of tail regenerates at different stages from 5 to 64 dpa. Wound epidermis covers the wound at 9-10 dpa. Early and late blastema is formed at 14 dpa and 25 dpa, respectively. Bl, blastemal; Mu, muscle; Ne, neural tube; No, notochord; WE, wound epidermis. Dashed line shows the amputation plane. Scale bar: 200 µm.

notochord, neural tube and muscles, appeared (Fig. 1E,F,L). At 64-73 days after amputation, the missing tail was almost completely restored (Fig. 1G,H,M).

To test cell apoptosis during regeneration, we performed a terminal deoxynucleotidyl transferase dUTP nick end labeling (TUNEL) assay on the wound-healing and blastemal stages. The assay revealed that at the wound-healing stage, cell apoptosis robustly occurred near the wound site as well as in the epithelium (Fig. 2A,B). In contrast, at the blastemal stage, less cell death was detected (Fig. 2C,D). This result showed that cell apoptosis mainly occurred at the wound-healing stage.

To test whether the blastemal cells in the tail regenerates of amphioxus are actively undergoing cell division, bromodeoxyuridine (BrdU) labeling on the tail regenerates at the blastemal stage was conducted. It was found that the cells within the blastema were actively dividing, which was similar to observations during vertebrate epimorphosis regeneration (Fig. 2E,F). Collectively, all the above data indicate that the tail regeneration of amphioxus *B. japonicum* is a vertebrate-like epimorphic process, as observed in amphioxus *B. lanceolatum* (Somorjai et al., 2012a).

De novo assembly of amphioxus transcriptome and gene annotation

To explore systematically the molecular mechanism underlying the tail regeneration process, we carried out transcriptome analysis of the tail regenerates at different stages (Fig. 3), using intact tails as controls.

After RNA sequencing, the low-quality raw sequences were removed through a strict evaluation, and the remaining short reads were assembled in a *de novo* process using Trinity software. In total, we obtained 101,406 expressed genes. The N50 was 1222 bases long, and the maximum length was 31,338 bases and the minimum length was 300 bases, with an average length of 892 bases.

For basic annotation of the assembled unigenes, sequence similarity searches against various protein databases were performed with an E-value threshold of 10^{-5}. It revealed that 47,876, 32,363, 27,380 and 24,609 unigenes had significant similarities to known genes or proteins in the Nr, SwissProt, KOG and KEGG databases, respectively (Fig. S1A). There were still 54,255 unigenes that could not be matched to already known genes, which may be partly caused by the presence of relatively short sequences (28,989 unigenes are ~300-399 bp long; 28.18%). Therefore, of the 102,868 unigenes, 48,613 (47.26%) unigenes were successfully annotated.

It is well known that transcription factors (TFs) play crucial roles in various biological processes, such as embryonic development and tissue regeneration. We aligned the protein sequences predicted from the unigenes to the TF database (plant TFdb/animal TFdb; http://bioinfo.life.hust.edu.cn/AnimalTFDB/#!/) and found that 1370 genes were assigned into 69 TF families, and the top 10 unigenes belonged to zf-C2H2, homeobox, bHLH, HMG, TF_bZIP, MYB, THAP, Fork head and THR-like families (Table S1, Fig. S1B). These annotations provide a valuable and rich resource for investigating specific processes, functions and pathways in amphioxus tail regeneration research.

Analysis of differentially expressed genes (DEGs)

To investigate the implicated genes at specific regenerative stages of tail regeneration, the expression levels of genes among different groups were compared. Pearson correlation analyses of gene expression between two samples of the same regeneration stage were close to 1 (from 0.9617 to 0.9967), whereas they were much lower between the two samples from different regeneration stages

Development (2019) 146, dev166017. doi:10.1242/dev.166017

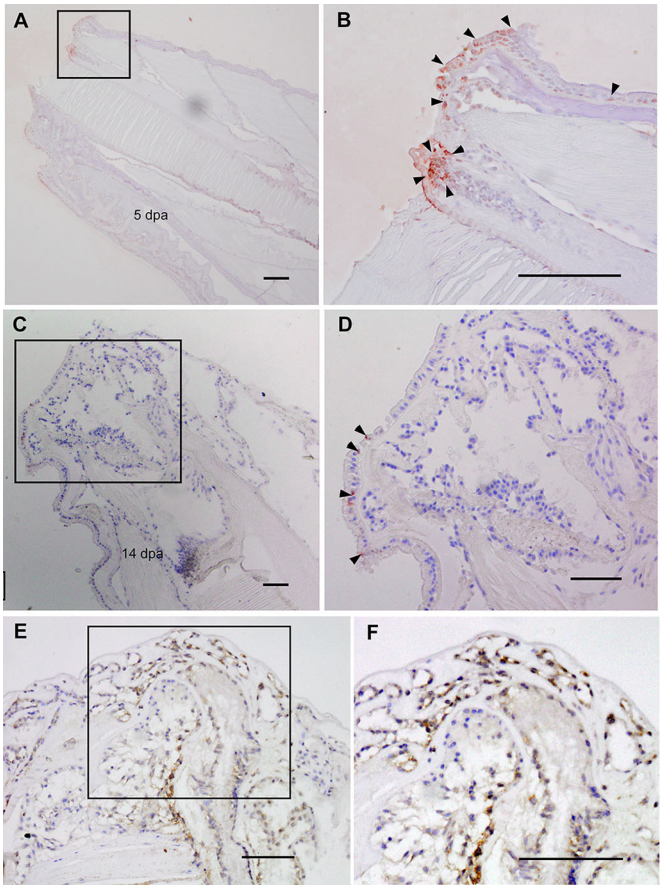

Fig. 2. Cell apoptosis and proliferation during tail regeneration process in amphioxus. (A-D) TUNEL assay of apoptosis. (A,B) At the wound-healing stage (5 dpa), strong apoptosis was detected (arrowheads) at the wound region. The boxed area in A is enlarged in B. (C,D) At the blastemal stage (14 dpa), very weak apoptosis was detected. The boxed area in C is enlarged in D. Arrowheads point to positive staining (red). (E,F) BrdU labeling assay of cell proliferation showing that active cell proliferation occurs in blastemal cells at the blastemal stage. The boxed area in E is enlarged in F. Positive signals are shown in brown and the sections were counterstained with Hematoxylin. Scale bars: 200 µm.

(Fig. S2), suggesting that there was excellent experimental reproducibility between two replicates of the same stage.

It was found that dramatic variation in the numbers of DEGs existed among the different groups (Fig. S3, Tables S2-S5). For example, when compared with intact tails, at the early wound-healing stage [at 14 hours post-amputation (hpa)], 5320 genes were upregulated and 13,786 were downregulated (Fig. S3A,B). In contrast, only relatively few DEGs were found between two groups representing two adjacent stages, such as the minimum number of DEGs observed between 15-day and 25-day groups (Fig. S3A,B).

To understand better the function of DEGs involved in different regeneration stages, we subjected the DEGs between two stages to gene ontology (GO) and KEGG analysis. Generally, it was shown that DEGs were enriched in many biological processes and signaling pathways, reflecting a high complexity of the molecular mechanism underlying the regeneration process.

Compared with those for the intact tail, the upregulated DEGs at the early wound-healing stage (14 hpa) were significantly enriched in 65 biological processes (P<0.05), including wound healing (GO:0042060), response to wounding (GO:0009611), extracellular structure organization (GO:0043062), tissue homeostasis (GO:0001894), regulation of responses to external stimuli (GO:0032101), response to stress (GO:0006950), cellular response to cytokine stimulus (GO:0071345), multicellular organismal process (GO:0032501), vasculature development (GO:0001944) (Table S6). Interestingly, in comparison with the intact tail, the upregulated DEGs at 5 days post-amputation (dpa) (late wound-healing stage) were remarkably enriched in 28 biological processes, of which ten related to defending the organism against external assaults, i.e. endocytosis (GO:0006897), response to other organism (GO:0051707), response to bacterium (GO:0009617), immune system process (GO:0002376), response to external biotic stimulus (GO:0043207), response to biotic stimulus (GO:0009607), response to fungus (GO:0009620), defense response to bacterium (GO:0042742), defense response (GO:0006952), and defense response to other organisms (GO:0098542) (Table S7). Fig. 4A and Table S8 show the expression level of DEGs enriched in GO biological process terms related to wound healing and the defense response. It was found that most genes involved in the two processes showed the lowest expression levels in the intact tails, but the highest expression levels in the tail regenerates at 14 hpa (early wound-healing stage) and medium expression levels in the tail regenerates at 5 dpa (late wound-healing stage). This pattern of gene expression suggested that these genes play crucial roles in the wound-healing process. It was also interesting to note that seven of the upregulated genes were assigned to the reactive oxygen species metabolic process (GO:0072593) (Fig. 4A, Table S8). This showed that reactive oxygen species might play a role during the tail regeneration of amphioxus, providing additional support to the recent observation that *Xenopus* tadpole tail amputation induced the production of reactive oxygen species (Love et al., 2013).

Compared with those for the intact tail, upregulated genes at the blastemal stage (15 dpa) were mainly classified into 19 items, two of which were cell cycle-related, the cell cycle (GO:0007049) and the regulation of cell cycle (GO:0051726) (Table S9), and upregulated genes at 25 dpa were markedly enriched in 24 biological processes, three of which were circulatory system process (GO:0003013), multicellular organismal process (GO:0032501) and multicellular organismal homeostasis (GO:0048871) (Table S10). In Fig. 4B and Table S11, all 75 genes showed a high percentage of enrichment in GO biological process terms related to cell cycles. Compared with the intact tail, the expression level of most genes related to the cell cycle were highly upregulated in tail regenerates at the blastemal stages (15 dpa and 25 dpa), of which the genes with the highest expression levels were concentrated at the blastemal stage of 15 dpa (Fig. 4B). This suggested that cell proliferation was active at the blastemal stages. The expression patterns of the genes also corroborated the results of BrdU labeling assays for cell proliferation in tail regeneration (Fig. 2E,F).

KEGG analysis revealed that, compared with the intact tail, the upregulated genes in the regenerative stages were enriched in many well-known signaling pathways that function in development and regeneration processes, including Wnt, Hedgehog, Jak-STAT, Notch, NOD-like receptor, hippo signaling pathways (Fig. S4A-D, Tables S12-S15). Of these signaling pathways, hippo signaling was recently shown to be implicated in regeneration, and Yap (the effector of the Hippo signaling cascade) is required for limb bud and tail regeneration in *Xenopus* tadpole (Hayashi et al., 2014a,b). We further verified the expression patterns of *yap* during the tail regeneration process in amphioxus by RNA *in situ* hybridization, which showed that *yap* is mainly expressed at the wound-healing stage in wound regions (Fig. S5A,B), and its expression is very weak at the blastema stage (Fig. S5C).

Development (2019) 146, dev166017. doi:10.1242/dev.166017

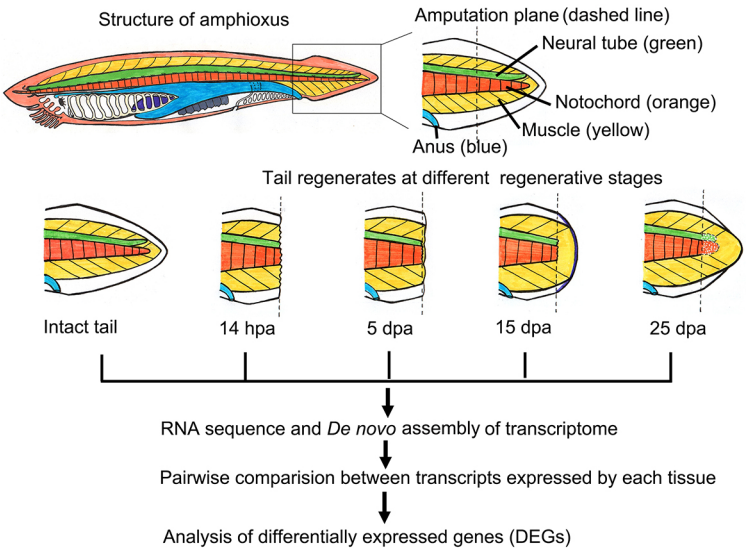

Fig. 3. Diagram of the strategy for obtaining a transcriptome of amphioxus related to its tail regeneration. Transcriptome analysis of the intact tails and tail regenerates at different regeneration stages from 14 hpa to 25 dpa. Dashed line shows the amputation plane.

bmp2/4 is expressed in wound sites at the wound-healing stage and is inducible by wounds

From the data on gene expression during regeneration, *bmp2/4* and other key genes of the BMP signaling pathway, including *receptorI*, *receptorII*, *smad1* and *smad4*, were found to be involved in the regeneration process of the amphioxus tail. BMP signaling is an evolutionarily conserved signaling pathways involved in development and regeneration processes (Slack, 2017). In European amphioxus, it was proposed that this signaling pathway is involved in tail regeneration, based on the finding that *msx* (a target gene of BMP signaling) is expressed during the tail regeneration process (Somorjai et al., 2012a). Whether BMP signaling plays important roles or not in the regeneration of amphioxus was of particular interest to us.

To understand the role of *bmp2/4* during the regeneration, its expression pattern was first examined systematically at different regeneration stages. It was evident that *bmp2/4* is specifically expressed in muscle cells in the wound sites at the wound-healing stage (Fig. 5A,B,E), but only very low expression signals were detected in blastema cells at the blastemal stage (Fig. 5C,F). This expression pattern change was also confirmed by qPCR, which revealed that *bmp2/4* was highly expressed at the wound-healing stage, but its expression levels decreased dramatically when the regeneration entered the blastemal stage (Fig. 5G).

To test whether BMP2/4, as a secreted protein, was also located in the wound region at the early regeneration stage, BMP2/4 was expressed in *Escherichia coli* cells and purified (Fig. S6). The purified protein was used to prepare a polyclonal antibody against BMP2/4, which was then used to conduct immunohistochemical staining. It was found that that BMP2/4 was mainly distributed in the muscle and neural tube cells in the wound region at the wound-healing stage (Fig. 5H), providing additional support to the finding that *bmp2/4* was specifically expressed in wound sites at the wound-healing stage.

We then tested whether the expression of *bmp2/4* was inducible by common wounds. For this purpose, transverse amputation and other injuries, such as hole puncture and scratching, were also induced, and the expression of *bmp2/4* was examined with *in situ* hybridization at different time points after wounding (0-8 h). It was found that *bmp2/4* was expressed in the wound sites and the regions near the wounds in all cases (Fig. 5I-K,M-O), suggesting that *bmp2/4* expression could be induced by wounds.

BMP2/4 knockdown impaired tail regeneration and increased cell apoptosis

We next designed an antisense morpholino (MO) of BMP2/4 and knocked down its expression by microinjection of the MO into the wound region of freshly amputated animals. Western blot revealed that the MO effectively knocked down the target gene expression *in vivo* (Fig. 6H). After inhibition of BMP2/4, the major phenotype is that the wound regions of all the tails (40) were jagged, did not heal and eventually decayed (Fig. 6E-G). Conversely, most animals that were given control MO passed the wound-healing stage (34 out of 40) and successfully produced blastema (Fig. 6A-D). This suggested that BMP2/4 is required for wound healing after amputation, and therefore the BMP2/4 knockdown impaired tail regeneration.

To gain insight into the mechanism of BMP2/4 function during regeneration, we investigated whether BMP2/4 regulated cell apoptosis at the early regeneration stage. Cell apoptosis between the control and the gene knockdown groups was compared. It was clear that BMP2/4 knockdown resulted in an increase of muscle and notochord cells undergoing apoptosis (Fig. 6I,J) and the average number of the positive muscle and notochord cells was 115 per section (estimated from four sections). In the control section, this number was 14 (estimated from four sections). This suggests that cell death is a possible reason for the failure of tail regeneration after BMP2/4 knockdown.

To test whether BMP2/4 plays a role during tail regeneration after wound healing, although it is expressed weakly at the blastema stage, we also knocked down its expression by microinjection of the MO into the early formed blastema of the 13-dpa amphioxus. The prominent phenotype is that, compared with the controls (Fig. S7A-C), the blastema of all the animals (14) grew toward the ventral side of their body (Fig. S7E). This suggested that BMP2/4 is necessary for the patterning of blastema growth. Subsequently, the abnormal ventral-folded tail blastema became adjusted to the midline of the body (Fig. S7F), similar to the blastema in normal regeneration (Fig. S7F), which may be due to the transient effect of the MO and their strong ability of self-regulation during regeneration.

BMP signaling is involved in tail regeneration

Although other BMP signaling pathway genes were found to be differentially expressed in the transcriptome analysis, we still cannot draw the conclusion that BMP signaling is involved in the

Development (2019) 146, dev166017. doi:10.1242/dev.166017

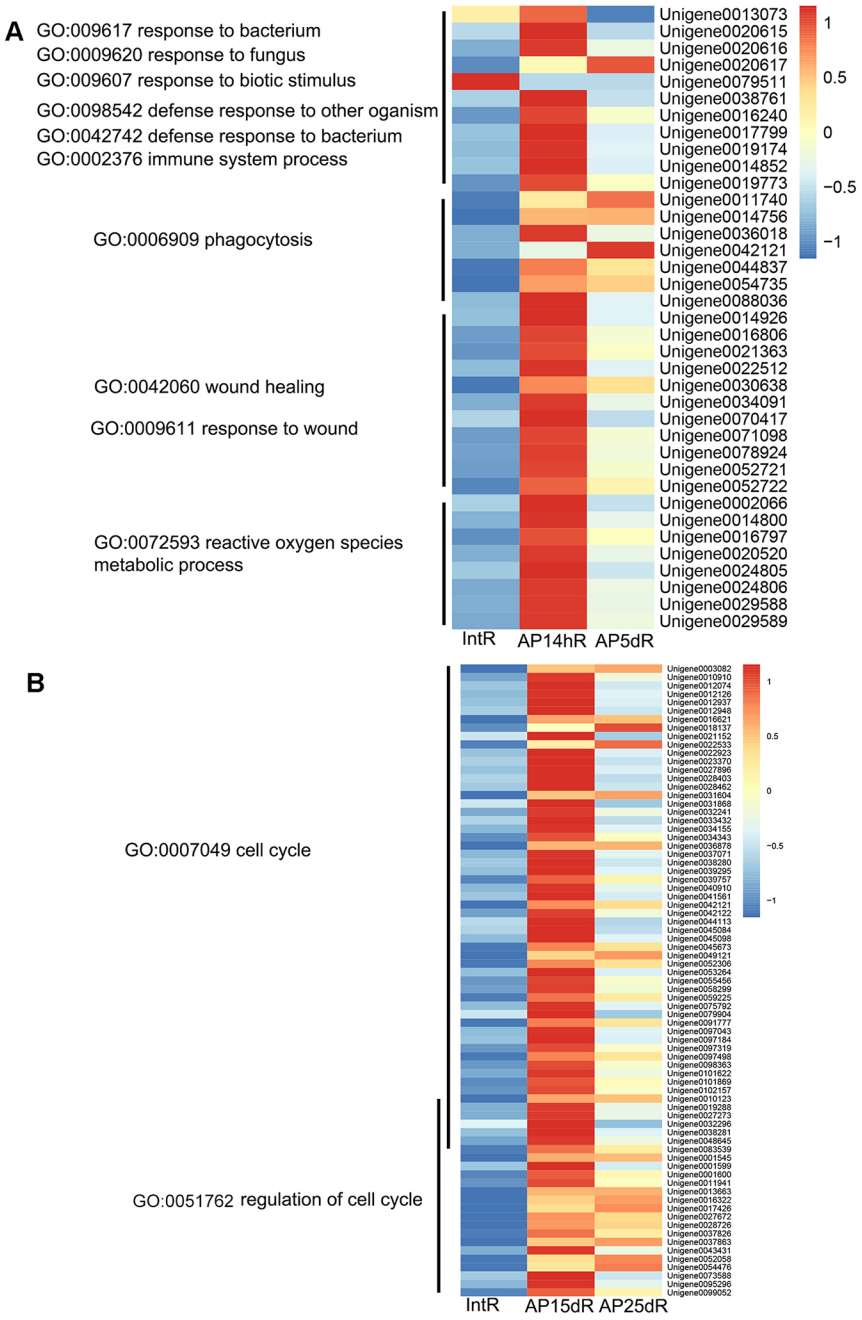

Fig. 4. Expression levels of DEGs of tail regenerates at different regenerative stages. (A) Heat map showing the expression levels of DEGs of tail regenerates at the wound-healing stage. The DEGs were enriched in GO biological process terms related to wound healing, defense response and reactive oxygen species metabolic processes. Detailed information regarding these DEGs is given in Table S4. (B) Heat map showing the levels of DEGs of tail regenerates at the blastemal stage. DEGs were enriched in GO biological process terms related to the cell cycle. Detailed information regarding these DEGs is given in Table S7.

regeneration process. To clarify this, the expression patterns of the other related genes, such as *receptorI*, *receptorII*, *smad1* and *smad4*, in addition to *bmp2/4*, were detected by *in situ* hybridization during the regeneration process. It was evident that at the wound-healing stage, all the genes examined showed spatial expression patterns similar to those of *bmp2/4* (Fig. S8A-P). The overlapping expression sites indicate that BMP signaling is actively involved in the regeneration. To further examine the role of BMP signaling, Noggin (a natural inhibitor of BMP signaling)-gel beads were implanted immediately after tail amputation (Fig. 7A-F). At 24 h after bead implantation, approximately half of the animals (46 of 100) rejected the beads into water, and the remaining beads were kept in the tissues near the wound region at 6 days after implantation. Of these animals, most of their tails (43 of 46) became decayed, and only a few had remaining tails (Fig. 7D-F). In contrast, most control animals (45 out of 60) formed blastema similar to the process of normal regeneration (Fig. 7A-C). Therefore, when BMP signaling was blocked, the animals were unable to pass through the wound-healing stage and failed to form blastema (Fig. 7D-F), indicating that BMP signaling is required for tail regeneration.

DISCUSSION

Regeneration exists widely and non-uniformly across the Metazoa, but the view that regeneration is an ancestral trait is still a hypothesis (Slack, 2017). The cephalochordate amphioxus, the most basal living chordate, provides an opportunity to explore evolution of regenerative mechanisms in chordates from the invertebrate to vertebrate transition. However, many questions regarding tail regeneration in amphioxus are still unclear. Previous studies of tail regeneration in European amphioxus showed that amphioxus

Development (2019) 146, dev166017. doi:10.1242/dev.166017

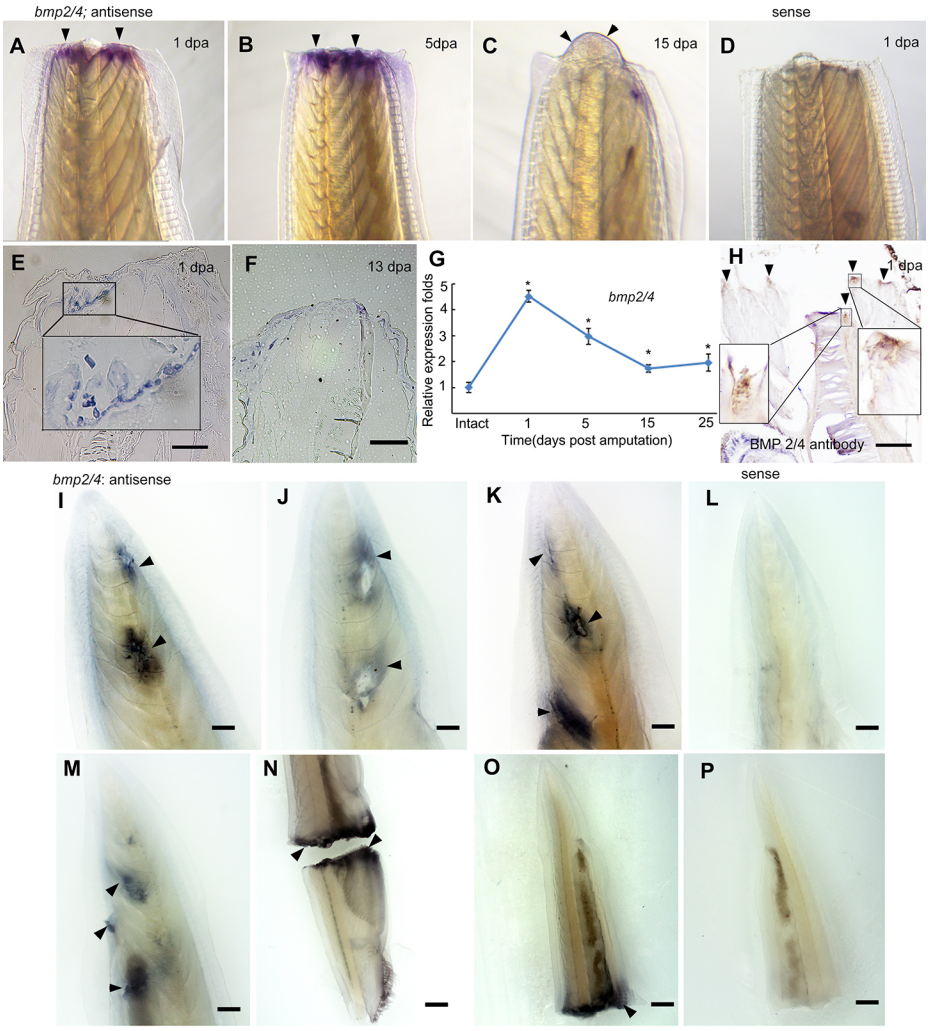

Fig. 5. Expression patterns of *bmp2/4* during the tail regeneration process. (A-D) Whole-mount *in situ* hybridization analysis of *bmp2/4* expression during the tail regeneration process. (A,B) *bmp2/4* is highly and specifically expressed in the wound region at the wound-healing stage. (C) *bmp2/4* is expressed in the blastema at a relatively low level at the blastema stage. (D) No positive staining signals were detected in the control (sense probe). Arrowheads point to the positive staining (in blue) for *bmp2/4* expression. (E,F) *In situ* hybridization analysis of *bmp2/4* expression on tissue sections of tail regenerates at the wound-healing stage (E) and early blastema stage (F). (G) q-PCR analysis of *bmp2/4* expression during the tail regeneration process. 'Intact' on the *x*-axis means intact tail, which was used as control. Data are expressed as mean ±s.d. (n=3). *P<0.01 (compared with intact digit). (H) Immunostaining of BMP2/4 on a tissue section at the wound-healing stage. Arrowheads point to the positive staining (brown). Boxed areas are enlarged in insets. (I-P) Whole-mount *in situ* hybridization analysis of *bmp2/4* expression after generation of wounds. (I,J,K,M) *bmp2/4* is expressed in or near the wound site immediately (ipp), at 1, 4 and 8 h post-puncture (hpp). (N,O) *bmp2/4* is expressed in or near the wound site immediately post-amputation (ipa) at different levels. (L,P) No staining was detected in negative controls (replaced antisense probes with sense probes). Arrowheads point to the positive signaling staining (blue). Tails are oriented with distal towards the top. Scale bars: 200 µm.

tail regeneration proceeds as an epimorphic process, which is similar to vertebrates, based on the fact that regeneration occurs at the bulb-like blastema that forms from the stump after amputation (Somorjai et al., 2012a). In contrast, it was claimed that the cirri regeneration in Asian amphioxus occurs via 'morphallaxis', as no active cell proliferation was detected during the regeneration process (Kaneto and Wada, 2011). Our study clearly demonstrated that tail regeneration in amphioxus *B. japonicum* is an epimorphosis process similar to that in vertebrates and showed that active cell proliferation was evident during the tail regeneration process (Fig. 2F).

In this study, it was also observed that there is a clear difference between the wound-healing processes of tail regeneration in amphioxus *B. japonicum* and vertebrate limb or tail regeneration. In amphibians, after limb or tail amputation, the wound surface is covered very quickly by the migrated epithelial cells, usually within 24 h or even 5 h post-amputation (Repesh and Oberpriller, 1978). In zebrafish, upon caudal fin amputation, epidermis cells cover the wound and repair it rapidly within several hours (Li et al., 2015). In comparison, the wound-healing process of tail amputation in amphioxus *B. japonicum* is longer, and the wound site remains unclosed or uncovered for more than one week. Unexpectedly, our observation is also different from that in European amphioxus, which can close the wound within 1-2 days after amputation (Somorjai et al., 2012a). However, this is an interesting phenomenon in which the amputated animals are seldom infected by pathogens during the long healing process. *De novo* transcriptome analyses of intact tail and tail regenerates at different stages and the identification of a batch of DEGs between different tissues reveal that a large number of these DEGs are related to transcription factors, signaling pathways and various biological processes, some of which are implicated in the developmental process. This provides many clues to exploring the cellular and molecular events that occur during the regeneration process. When comparing the gene expression levels of the intact tails with those of tail regenerates at the wound-healing stage, it was observed that a large number of highly upregulated genes are grouped into immune response, defense, and wound-healing processes. This explains how amphioxus can protect themselves from infection by pathogens when undergoing long periods of wound healing.

Previously, there had been no functional study of genes in the regeneration process in amphioxus. In this study, for the first time, we successfully knocked down the expression of BMP2/4 by vivo-morpholino and blocked BMP signaling by grafting Noggin-soaked beads. We found that BMP2/4 and related signaling pathway components are essential for the process of tail regeneration. The involvement and indispensable role of BMPs or BMP signaling in regeneration appears to be conserved across metazoans. In planarians, the *bmp2/4-like* and *smad4-like* genes are necessary for lateral regeneration (Reddien et al., 2007). Similarly, in fish, the BMP signaling pathway is required for caudal fin regeneration, and

Development (2019) 146, dev166017. doi:10.1242/dev.166017

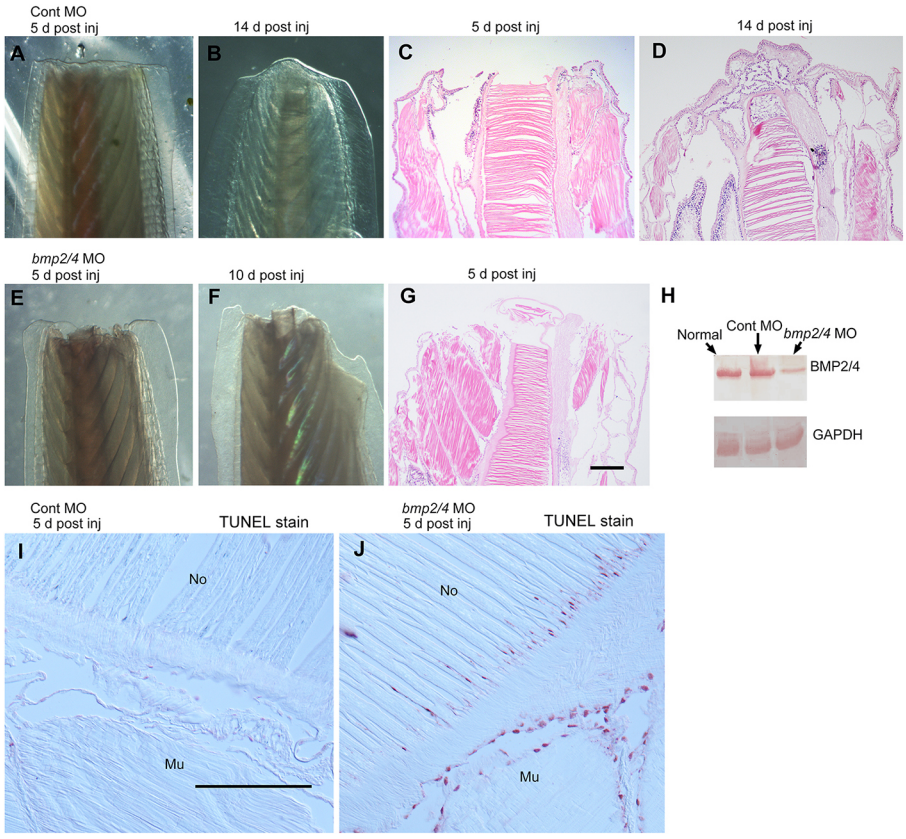

Fig. 6. Vivo-morpholino-mediated BMP2/4 knockdown impairs tail regeneration. (A-D) Tail regenerates and their tissue sections at different time points post-injection (post inj) of control MO. The tail underwent a normal regenerative process characterized by the formation of a blastema. (E-G) Tail regenerates and their tissue sections at different time points post-injection of *bmp2/4* MO. The MO inhibits regeneration, resulting in the decay of regenerates. (H) Confirmation of morpholino-mediated gene knockdown by western blot. (I,J) TUNEL assay of apoptosis in tail regenerates at 5 days post-injection of *bmp2/4* MO. (I) In tail regenerates injected with control MO, very weak apoptosis was detected in the muscle (Mu) and notochord (No). (J) In tail regenerates injected with *bmp2/4* MO, strong positive staining for apoptosis (red) was detected in the muscle and notochord. Scale bars: 100 µm.

ectopic expression of the BMP signaling inhibitor Chordin can perturb the normal regeneration process (Smith et al., 2006; Thorimbert et al., 2015; Rajaram et al., 2017). In amphibians, BMP is involved in both tail and limb regeneration (Beck et al., 2006). Moreover, in mammals, such as mice, it has been found that the BMP signaling pathway is indispensable for digit regeneration (Han et al., 2008), and the function of BMP signaling in regeneration is further highlighted by the fact that exogenous BMP2 or BMP7 carried by gel beads can induce digit regeneration from non-regenerating proximal amputation (Yu et al., 2010).

In addition to being expressed instantly after amputation, we also found an interesting feature about *bmp2/4* expression in amphioxus:

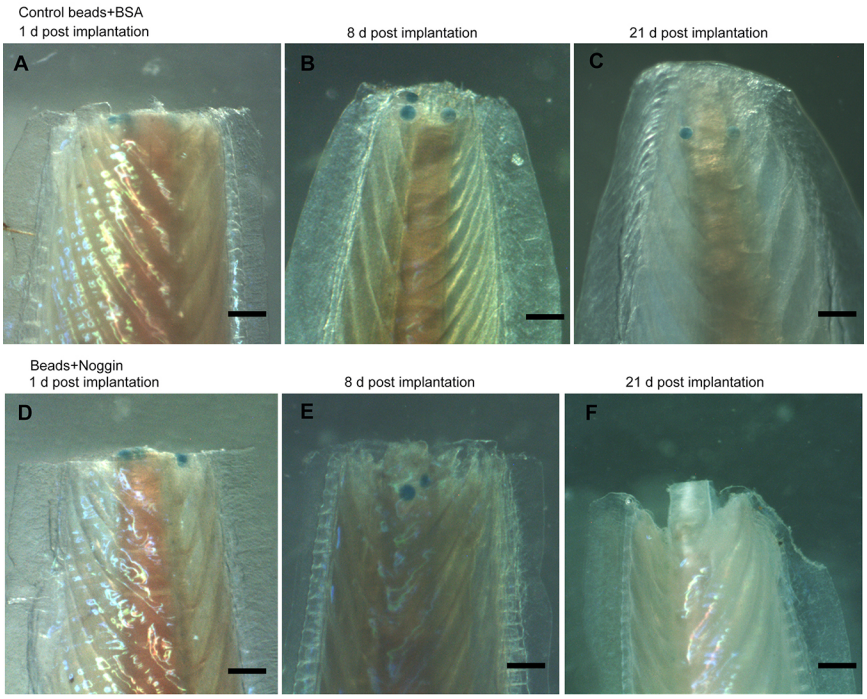

Fig. 7. Inhibition of BMP signaling by Noggin-bead implantation during the tail regeneration process. (A-C) Tail regenerates at 1, 8 and 21 days post-implantation of control beads. The tail underwent a normal regenerative process characterized by the formation of a blastema. (D-F) Tail regenerates at 1, 8 and 21 days post-implantation of Noggin-beads. The Noggin-beads impair regeneration, resulting in the decay of regenerates. Scale bars: 200 µm.

Development (2019) 146, dev166017. doi:10.1242/dev.166017

bmp2/4 expression is inducible by general wounds. In the crinoid *Antedon bifida*, a similar species, *Anbmp2/4,* a vertebrate *bmp2/4* homolog, is involved in arm regeneration. Compared with *bmp2/4* expression in amphioxus, *Anbmp2/4* is also expressed at the early regeneration stage (repair phase), but its expression signals are not detectable less than 24 h after amputation (Patruno et al., 2003). This finding suggests that *bmp2/4* can be regarded as a biomarker of wounds in amphioxus.

Novel findings of this study are that *bmp2/4* is immediately induced by wounding and that BMP signaling is required for wound healing after amputation. In contrast, in epimorphic regeneration of other species, the roles of BMP signaling are mainly related to cell proliferation (Ricci and Srivastava, 2018; Wagner et al., 2017). It is noticeable that in European amphioxus, *msx* (a target gene of BMP signaling) is expressed in the mesenchyme of the blastema (Somorjai et al., 2012a), combining the expression patterns of BMP signaling genes during tail regeneration of *B. japonicum* shown by us (Fig. 5C, F, Fig. S8), suggesting that BMP signaling may play a role at the blastema stage. One role of BMP2/4 at the blastema stage that was found by us is that it regulates the patterning of blastema growth, but the underlining mechanism needs to be addressed.

The cellular basis of tail regeneration in amphioxus is still not well defined. Here, we show that two basic aspects of cellular events, cell apoptosis and cell proliferation, are involved in the tail regeneration of amphioxus, resembling vertebrate regeneration. However, the cellular origin of the blastema in amphioxus tail regeneration remains elusive. In limb regeneration in salamanders, blastemal cells are heterogeneously derived from satellite cells and cells dedifferentiated from various cells in stumps, but the relative percentages are not yet clear (Morrison, et al., 2006; Kragl et al., 2009). In planarian regeneration, stem cells (neoblasts) appear to be the sole cell origin of the blastema (Tanaka and Reddien, 2011). Previous studies regarding the tail regeneration of amphioxus proposed that satellite cells are one source of the blastema, based on the expression of the muscle stem cell marker gene *pax3/7* in blastema (Somorjai et al., 2012a). It is clear that the information currently available regarding the cellular origin of the blastema in tail regeneration is still limited. To address this question and other cellular events during regeneration, effective cell labeling or tracing techniques must be developed in amphioxus.

In summary, our study highlights the cellular and molecular basis of tail regeneration in amphioxus by detailed morphological, molecular and transcriptome analyses, confirming that amphioxus tail regeneration is a vertebrate-like epimorphosis process. The identification of the BMP signaling pathway in regeneration provides a basis for addressing the function of genes during the tail regeneration in amphioxus. Generally, our data provide new evidence for the ancestral nature of whole-body regeneration (Slack, 2017). Our results and the previous works regarding regeneration in amphioxus will certainly promote future detailed studies on how amphioxus regenerates its tail.

MATERIALS AND METHODS

Animal collection, amputation and care

Amphioxus (*Branchiostoma japonicum*) were collected from the 'amphioxus ground' in the vicinity of Qingdao and cultured in tanks with aerated seawater under a natural light-dark period and at ambient temperature. Animals with body length of approximately 3 cm were collected and amputated with a razor blade approximately 1 mm posterior to the anus. After amputation, the animals were kept in a tank with running aerated seawater and fed with single-celled algae from the third day onward.

Morphological and histological observations

Regeneration of the amputated tail was observed and photographed under an Olympus stereomicroscope (ZSX12) daily. The tail regenerates at different regeneration stages were collected and fixed in freshly prepared 4% paraformaldehyde (PFA) in PBS. They were then dehydrated in ethanol, embedded in paraffin and sectioned longitudinally at 8-µm thickness. The sections were stained with Hematoxylin and Eosin (Sigma-Aldrich) and photographed under a Zeiss microscope (AX10).

RNA isolation, Illumina paired-end sequencing and *de novo* assembly

The intact tails and tail regenerates at different regeneration stages (cut at the level of the anus) were used for total RNA extraction with Trizol regent (Invitrogen). mRNAs were enriched by magnetic beads combining the oligo (dT) and the purified mRNA fragmented by the addition of the fragmentation solution (100 mM $ZnCl_2$ in 100 mM Tris-HCl, pH 7.0). The fragmented mRNA was reverse transcribed to first strand cDNA with transcriptase (Invitrogen), random hexamers and dNTP. The second strand of cDNA was prepared by the addition of the reaction buffer containing dNTPs, RNase H and DNA polymerase I. The cDNA fragments were then purified with a QiaQuick PCR extraction kit and subjected to the end repair process by the addition of a single 'A' base and the ligation of Illumina sequencing adapters. The ligation products were selected by agarose gel electrophoresis, amplified by PCR, and sequenced using Illumina HiSeq 4000 by Gene Denovo Biotechnology Co. (Guangzhou, China). Through a strict filtration (the reads containing adapters, the reads containing Ns and the low-quality reads were removed), high-quality clean reads were obtained and assembled in a *de novo* process using Trinity software, consisting of three software modules: Inchworm, Chrysalis and Butterfly (Grabherr et al., 2011). The reads were assembled into contigs by the Inchworm program, the minimum overlapping contigs were clustered into sets of connected components by the Chrysalis program, and then the transcripts were constructed by the Butterfly program. The longest transcript of each cluster was termed as 'unigene' thereafter, and the unigene library for the species was established and employed in subsequent analysis. The coding regions of the unigenes were predicted by EMBOSS Getorf Software (http://emboss.bioinformatics.nl/cgi-bin/emboss/getorf).

Gene annotation

The unigene annotation was performed using local BLAST programs against NCBI non-redundant (nr) protein, Swiss-Prot/TrEMBL, Clusters of Orthologous Groups (COG/KOG), Gene Ontology (GO) and Kyoto Encyclopedia of Genes and Genomes (KEGG) databases.

Identification of DEGs

The abundances of genes were calculated and normalized by the RPKM (reads per kb per million reads) method (Mortazavi et al., 2008). To identify DEGs across groups, the edgeR package (http://www.r-project.org/) was used. Genes with a fold change ≥2 and a false discovery rate (FDR)<0.05 in a comparison were regarded as significantly differentially expressed. DEGs were then subjected to enrichment analysis of GO functions, COG/KOG and KEGG pathways.

TUNEL staining

To detect cell apoptosis during the tail regeneration, TUNEL staining was performed on sections of tail regenerates at the wound-healing and blastema-formation stages, respectively. The tail regenerates were collected at 5 and 20 dpa, fixed in 4% PFA in PBS and 8-µm-thick paraffin sections were prepared following the protocol described above. Using an *in situ* cell death detection POD kit (Roche), the sections were TUNEL stained in accordance with the manufacturer's instructions. In brief, paraffin sections were dewaxed in xylene and permeabilized using Proteinase K (20 µg/ml) in 10 mM Tris-HCl for 10 min, followed by treatment with 0.3% H_2O_2 in methanol at room temperature for 10 min to quench endogenous peroxidase. After rinsing with PBS, sections were incubated with converter-POD at 37°C for 30 min, and then reacted with 3-amino-9-ethylcarbazole (AEC). The sections were counterstained with Mayer's Hematoxylin.

Development (2019) 146, dev166017. doi:10.1242/dev.166017

BrdU labeling

To detect cell proliferation during the blastemal stage, 5-bromo-2-deoxyuridine (BrdU, Sigma) labeling was performed on tail regenerates at 15 dpa. BrdU (20 µg/ml in PBS) was microinjected into the region of the blastema of tail regenerates under a stereomicroscope. The microinjection was performed twice with a 14-h gap between each injection. The total volume of the BrdU solution for injection was approximately 400-600 nl per animal. Tail regenerates were collected 4 h after the second microinjection and fixed with freshly prepared 4% PFA. After thorough washing with PBS, the fixed tissues were immersed in 30% sucrose in PBS at 4°C overnight, embedded with Tissue-Tek and cryosectioned at a thickness of 12 µm. The sections were then rinsed with PBS, incubated in 2 N HCl at 37°C for 30 min to denature DNA, and neutralized in 0.1 M sodium borate for 15 min. The neutralized sections were incubated in 3% H_2O_2 at room temperature for 15 min to quench endogenous peroxidase activity, and then with 5% goat serum to block nonspecific binding. Subsequently, the sections were incubated with mouse anti-BrdU antibody (Abcam, ab8152) at a dilution of 1:100 at 4°C overnight. After washing four times with PBST [PBS containing 0.1% (v/v) Tween-20], sections were incubated with HRP-conjugated goat anti-mouse antibody (Promega, W4021) at a dilution of 1:400, reacted with DAB (3,3′-diaminobenzidine tetrahydrochloride) in the presence of 0.03% H_2O_2, and counterstained with Hematoxylin.

Expression, purification of BMP2/4 and antibody preparation

To prepare recombinant BMP2/4, the open reading frame of *B. japonicum bmp2/4* was amplified by PCR. The following primers were used: forward primer 5′-CGCGGATCCATGATTCCTGGTAACAGATC-3′ and reverse primer 5′-CCGCTCGAGACGGCACCCGCATCCTTC-3′ (underlined sequences show the *Bam*HI and *Xho*I restriction enzyme sites). After digestion with *Bam*HI/*Xho*I, the PET32-BMP2/4 plasmid was constructed by ligation of the amplification product into the expression vector PET 32a (+) (Novagen). Expression induction and protein purification were carried out as described by Liu and Zhang (2009). The BMP2/4 antiserum was prepared in rabbits following the method of Pathirana et al. (2016). The antibody in rabbit serum was purified with a HiTrap Protein G HP affinity purification column. The antibody was detected by traditional gel double immunodiffusion methods. A gel plate was prepared by melting 0.2 g agarose in 20 ml PBS and pouring this into a dish, into which seven wells were punched (one central well for antigen and six circumambient wells for antibody at different dilutions). Then the antigen (BMP2/4; 10 µl at a concentration of 1 mg/ml) and the antibody (diluted at 1:50, 1:100, 1:200, 1:400, 1:800; 1:1000, 1;1500) were loaded into the wells, respectively. The plate was incubated in a wet chamber at 30°C for more than 24 h. When precipitin lines could be clearly observed, the gel was stained with 0.5% (w/v) Coomassie Brilliant Blue R-250 (containing 40% ethanol, 10% glacial acetic acid and 50% H_2O) for 20 min. Then, destaining was conducted with destaining solution [15% (v/v) ethanol, 5% (v/v) glacial acetic acid, 80% H_2O) until the precipitin lines were maximally visible and the background staining was negligible.

Gene knockdown by vivo-morpholinos

To knock down the expression of BMP2/4 protein, the antisense vivo-morpholino (MO) oligonucleotides were designed and synthesized by Gene Tools, LLC (Philomath). The MO sequence was complementary to the 5′ sequence near the start of translation (ATG): 5′-GCAGCGATCTG-TTACCAGGAATCAT-3′. For control, a corresponding 5-mispair oligo (GaAGCcATCTcTTACCAcGAATaAT) for the MOs was designed (lower case letters indicate mis-pairs). After the tail amputation, the MOs were injected at a concentration of 15 µM into the tissues on the wound site at approximately 1-1.5 µl per animal. The regeneration process was then observed at different time points.

Western blot

To confirm the efficiency of MO knockdown, western blot was carried out on regenerates at 3 days post-injection. The tail regenerates were collected and homogenized with ice-cold tissue lysis buffer (50 mM Tris-HCl, 150 mM NaCl, 1 mM PMSF, pH 7.2), and centrifuged at 12,000 ***g*** at 4°C for 30 min. The supernatants were pooled and stored at −70°C until use. The protein concentration was determined by the Bradford method. The above samples of protein were prepared and run on a 12% sodium dodecyl sulfate-polyacrylamide gel electrophoresis (SDS-PAGE) gel with a 4% spacer gel using the buffer system of Laemmli (1970). The separated proteins on the gels were blotted on nitrocellulose membrane (Hybond, Amersham Pharmacia). After incubation with 3% defatted dry milk in PBS at room temperature for 1.5 h, the membrane was incubated with rabbit anti-amphioxus BMP2/4 antibody diluted 1: 400 at 4°C overnight. After washing in 20 mM PBS, the membrane was incubated with peroxidase-conjugated goat anti-rabbit IgG (Abcam, ab97051) diluted 1:1000 with PBS at room temperature for 45 min. Bands were visualized using 0.06% DAB in 50 mM Tris-HCl buffer (pH 7.6) and 0.03% H_2O_2.

Bead implantation

Blue Affi-gel beads (Bio-Rad, 153-7302) with a size of 80-150 µm (100-200 mesh) were used for the bead grafting experiment. The beads were washed repeatedly with PBS and then soaked in 10 µg/µl BMP antagonist mouse noggin (R&D Systems, 6697-NG-25) in PBS at 4°C overnight. Control beads were soaked in PBS or 0.1% bovine serum albumin in PBS. Bead grafting was carried out 2 h after tail amputation. After the amputation, a single bead that had absorbed noggin was picked up by a glass needle used for microinjection and carefully inserted into the amputation wound site under a stereomicroscope. Usually, an animal was implanted with two to four beads. The grafted beads could be readily seen under a stereomicroscope. After bead implantation, the tail regeneration process was checked at different time points.

Whole-mount *in situ* hybridization

To examine the expression patterns of BMP signaling genes during the regeneration process, whole-mount *in situ* hybridization was performed on tail regenerates according to the method of Campbell et al. (2011) with slight modifications. In brief, the collected tissues were fixed in freshly prepared 4% PFA at 4°C overnight, dehydrated and then stored in 100% ethanol at 20°C. Tissues were permeabilized with 5 µg/ml proteinase K (New England BioLabs) at 37°C for 15 min. Pre-hybridization was performed at 60°C overnight. The PGM-T-easy vectors (Promega) containing target genes were linearized with *Nco*I or *Xho*I, and the sense and antisense probes were *in vitro* transcribed with T7 or SP6 RNA polymerase and digoxigenin RNA labeling mix (Roche Applied Science). Hybridization was performed at 60°C for 24 h. Alkaline-phosphatase (AP)-conjugated anti-digoxigenin antibody (Roche Applied Science) incubation, at a dilution of 1:2000, was conducted at 4°C overnight. The colorimetric alkaline phosphatase reaction was developed with BCIP and NBT (Roche Applied Science).

In situ hybridization on tissue sections

To verify the expression patterns of *bmp2/4*, *in situ* hybridization was also conducted on tissue sections of tail regenerates. The sections were processed and hybridized as described by Fan et al. (2007).

Quantitative real-time PCR (qRT-PCR)

qRT-PCR was performed to verify the mRNA levels of *bmp2/4* at the different stages of tail regeneration. Total RNAs were isolated with Trizol (Roche Applied Science) from tail regenerates at different stages. Single-stranded cDNAs were synthesized with the reverse transcription system (Takara) according to the instructions of the manufacturer. Following quantification of the cDNA templates, qRT-PCR was performed using Power SYBR Green PCR Master Mix (Takara) on an ABI 7500 real-time PCR system (Applied Biosystems) as described previously (Wang and Zhang, 2011). Glyceraldehyde-3-phosphate dehydrogenase (GAPDH) was chosen as the internal reference for qRT-PCR standardization. Data were quantified using the $2^{-\Delta\Delta CT}$ method based on CT values (Livak and Schmittgen, 2011). The primers employed in this study were: GAPDH-Forward, GCCGATGTTCGTCATGGGTGTC; GAPDH-Reverse, GGTC-TTCTGCGTGGCGGTGTA; BMP2/4-Forward, GCTGCTCACATACA-CGGATG; BMP2/4-Reverse, CGAATGTCTCCTGCAGTTGG.

Immunohistochemistry

To detail the distribution of BMP2/4 at the wound site, immunohistochemical staining was also conducted on tissue sections of tail regenerates at the

wound-healing stage. Processing and immunostaining of the sections was conducted as described previously (Liang and Zhang, 2006). The primary antibody was diluted 1:400 and the secondary antibody (HRP-conjugated goat anti-rabbit IgG; Abcam, ab97051) was diluted 1:600.

Acknowledgements
We thank Dr Ting Liu for technical assistance with preparing tissue sections.

Competing interests
The authors declare no competing or financial interests.

Author contributions
Conceptualization: Y.L., S.Z.; Methodology: Y.L., D.R., S.H.; Validation: S.H., A.P.; Formal analysis: Y.L.; Investigation: Y.L., D.R., S.H., A.P., Q.X.; Data curation: A.P.; Writing - original draft: Y.L.; Writing - review & editing: Y.L., S.Z.; Visualization: Y.L., A.P.; Supervision: Y.L.; Project administration: Y.L.; Funding acquisition: Y.L., S.Z.

Funding
This work was supported by the Natural Science Foundation of Shandong Province (ZR2012CM030), the AoShan Program of Qingdao National Laboratory for Marine Science and Technology (2017ASTP01) and the Fundamental Research Funds for Central Universities (201762003, 201822018).

Data availability
The transcriptome analysis data sets are available at the NCBI Short Read Archive (SRA) with accession number PRJNA428418.

Supplementary information
Supplementary information available online at
http://dev.biologists.org/lookup/doi/10.1242/dev.166017.supplemental

References
Beck, C. W., Christen, B., Barker, D. and Slack, J. M. W. (2006). Temporal requirement for bone morphogenetic proteins in regeneration of the tail and limb of Xenopus tadpoles. *Mech. Dev.* **123**, 674-688.
Bely, A. E. (2006). Distribution of segment regeneration ability in the Annelida. *Integr. Comp. Biol.* **46**, 508-518.
Bely, A. E. and Nyberg, K. G. (2010). Evolution of animal regeneration: reemergence of a field. *Trends. Ecol. Evol.* **25**, 161-170.
Biberhofer, R. (1906). Über Regeneration bei *Amphioxus lanceolatus*. *Arch. EntwMech. Org.* **22**, 1517.
Campbell, L. J., Suárez-Castillo, E. C., Ortiz-Zuazaga, H., Knapp, D., Tanaka, E. M. and Crews, C. M. (2011). Gene expression profile of the regeneration epithelium during axolotl limb regeneration. *Dev. Dyn.* **240**, 1826-1840.
Dinsmore, C. E. (1991). *A History of Regeneration Research: Milestones in the Evolution of a Science*. Cambridge University Press.
Fan, C., Zhang, S., Liu, Z., Li, L., Luan, J. and Saren, G. (2007). Identification and expression of a novel class of glutathione-S-transferase from amphioxus Branchiostoma belcheri with implications to the origin of vertebrate liver. *Int. J. Biochem. Cell. Biol.* **39**, 450-461.
Goss, R. J. (1969). *Principles of Regeneration*. Academic Press.
Grabherr, M. G., Haas, B. J., Yassour, M., Levin, J. Z., Thompson, D. A., Amit, I., Adiconis, X., Fan, L., Raychowdhury, R., Zeng, Q. et al. (2011). Full-length transcriptome assembly from RNA-seq data without a reference genome. *Nat. Biotechnol.* **29**, 644-652.
Han, M., Yang, X., Lee, J., Allan, C. H. and Muneoka, K. (2008). Development and regeneration of the neonatal digit tip in mice. *Dev. Biol.* **315**, 125-135.
Hayashi, S., Ochi, H., Ogino, H., Kawasumi, A., Kamei, Y., Tamura, K. and Yokoyama, H. (2014a). Transcriptional regulators in the Hippo signaling pathway control organ growth in Xenopus tadpole tail regeneration. *Dev. Biol.* **396**, 31-41.
Hayashi, S., Tamura, K. and Yokoyama, H. (2014b). Yap1, transcription regulator in the Hippo signaling pathway, is required for Xenopus limb bud regeneration. *Dev. Biol.* **388**, 57-67.
Kaneto, S. and Wada, H. (2011). Regeneration of amphioxus oral cirri and its skeletal rods: Implications for the origin of the vertebrate skeleton. *J. Exp. Zoolog. B. Mol. Dev. Evol.* **316B**, 409-417.
Kragl, M., Knapp, D., Nacu, E., Khattak, S., Maden, M., Epperlein, H. H. and Tanaka, E. M. (2009). Cells keep a memory of their tissue origin during axolotl limb regeneration. *Nature* **460**, 60-65.
Laemmli, U. K. (1970). Cleavage of structural proteins during the assembly of the head of bacteriophage T4. *Nature* **227**, 680-685.
Li, Q., Yang, H. and Zhong, T. P. (2015). Regeneration across metazoan phylogeny: lessons from model organisms. *J. Genet. Genomics* **42**, 57-70.
Liang, Y. J. and Zhang, S. C. (2006). Demonstration of plasminogen-like protein in amphioxus with implications for the origin of vertebrate liver. *Acta Zool.* **87**, 141-145.
Liu, M. Y. and Zhang, S. C. (2009). A kringle-containing protease with plasminogenlike activity in the basal chordate Branchiostoma belcheri. *Biosc. Rep.* **29**, 385-395.
Livak, K. J. and Schmittgen, T. D. (2011). Analysis of relative gene expression data using real-time quantitative PCR and the $2^{-\Delta\Delta CT}$ method. *Methods* **25**, 402-408.
Love, N. R., Chen, Y., Ishibashi, S., Kritsiligkou, P., Lea, R., Koh, Y., Gallop, J. L., Dorey, K. and Amaya, E. (2013). Amputation-induced reactive oxygen species are required for successful Xenopus tadpole tail regeneration. *Nat. Cell Biol.* **15**, 222-228.
Morrison, J. I., Lööf, S., He, P. and Simon, A. (2006). Salamander limb regeneration involves the activation of a multipotent skeletal muscle satellite cell population. *J. Cell. Biol.* **172**, 433-440.
Mortazavi, A., Williams, B. A., McCue, K., Schaeffer, L. and Wold, B. (2008). Mapping and quantifying mammalian transcriptomes by RNA-Seq. *Nat. Methods* **5**, 621-628.
Pathirana, A., Diao, M., Huang, S., Zuo, L. and Liang, Y. (2016). Alpha 2 macroglobulin is a maternally-derived immune factor in amphioxus embryos: new evidence for defense roles of maternal immune components in invertebrate chordate. *Fish. Shellfish. Immunol.* **50**, 21-26.
Patruno, M., McGonnell, I., Graham, A., Beesley, P., Candia Carnevali, M. D. and Thorndyke, M. (2003). An bmp2/4 is a new member of the transforming growth factor-β superfamily isolated from a crinoid and involved in regeneration. *Proc. Biol. Sci.* **270**, 1341-1347.
Probst, G. (1930). Regenerationsstudien an Anneliden und *Branchiostoma lanceolatum* (Pallas). *Rev. Suisse. Zool.* **37**, 343-352.
Rajaram, S., Patel, S., Uggini, G. K., Desai, I. and Balakrishnan, S. (2017). BMP signaling regulates the skeletal and connective tissue differentiation during caudal fin regeneration in sailfin molly (*Poecilia latipinna*). *Dev. Growth Differ.* **59**, 629-638.
Reddien, P. W., Bermange, A. L., Kicza, A. M. and Sánchez Alvarado, A. (2007). BMP signaling regulates the dorsal planarian midline and is needed for asymmetric regeneration. *Development* **134**, 4043-4051.
Repesh, L. A. and Oberpriller, J. C. (1978). Scanning electron microscopy of epidermal cell migration in wound healing during limb regeneration in the adult newt, *Notophthalmus viridescens*. *Am. J. Anat.* **151**, 539-555.
Ricci, L. and Srivastava, M. (2018). Wound-induced cell proliferation during animal regeneration. *Wiley Interdiscip. Rev. Dev. Biol.* **7**, e321.
Silva, R. M. C. J., Mendes, E. G. and Mariano, M. (1998). Regeneration in the amphioxus (*Branchiostoma platae*). *Zool. Anzeiger.* **237**, 107-111.
Slack, J. M. W. (2017). Animal regeneration: ancestral character or evolutionary novelty? *EMBO. Rep.* **18**, 1497-1508.
Smith, A., Avaron, F., Guay, D., Padhi, B. K. and Akimenko, M. A. (2006). Inhibition of BMP signaling during zebrafish fin regeneration disrupts fin growth and scleroblast differentiation and function. *Dev. Biol.*. **299**, 438-454.
Somorjai, I. M. L. (2017). Amphioxus regeneration: evolutionary and biomedical implications. *Int. J. Dev. Biol.* **61**, 689-696.
Somorjai, I. M. L., Somorjai, R. L., Garcia-Fernàndez, J. and Escrivà, H. (2012a). Vertebrate-like regeneration in the invertebrate chordate amphioxus. *Proc. Natl. Acad. Sci. USA* **109**, 517-522.
Somorjai, I. M. L., Escrivà, H. and Garcia-Fernàndez, J. (2012b). Amphioxus makes the cut—again. *Commun. Integr. Biol.* **5**, 499-502.
Tanaka, E. M. and Reddien, P. W. (2011). The cellular basis for animal regeneration. *Dev. Cell.* **21**, 172-185.
Thorimbert, V., König, D., Marro, J., Ruggiero, F. and Jaźwińska, A. (2015). Bone morphogenetic protein signaling promotes morphogenesis of blood vessels, wound epidermis, and actinotrichia during fin regeneration in zebrafish. *FASEB J.* **29**, 4299-4312.
Vorontsova, M. A. and Liosner, L. D. (1960). *Asexual Propagation and Regeneration*. Pergamon Press.
Wagner, I., Wang, H., Weissert, P. M., Straube, W. L., Shevchenko, A., Gentzel, M., Brito, G., Tazaki, A., Oliveira, C., Sugiura, T. et al. (2017). Serum proteases potentiate BMP-induced cell cycle re-entry of dedifferentiating muscle cells during Newt limb regeneration. *Dev. Cell* **40**, 608-617.e6.
Wang, Y. and Zhang, S. C. (2011). Identification and expression of liver-specific genes after LPS challenge in amphioxus: the hepatic cecum as liver-like organ and “pre-hepatic” acute phase response. *Funct. Integr. Genomics* **11**, 111-118.
Yu, L., Han, M., Yan, M., Lee, E.-C., Lee, J. and Muneoka, K. (2010). BMP signaling induces digit regeneration in neonatal mice. *Development* **137**, 551-559.

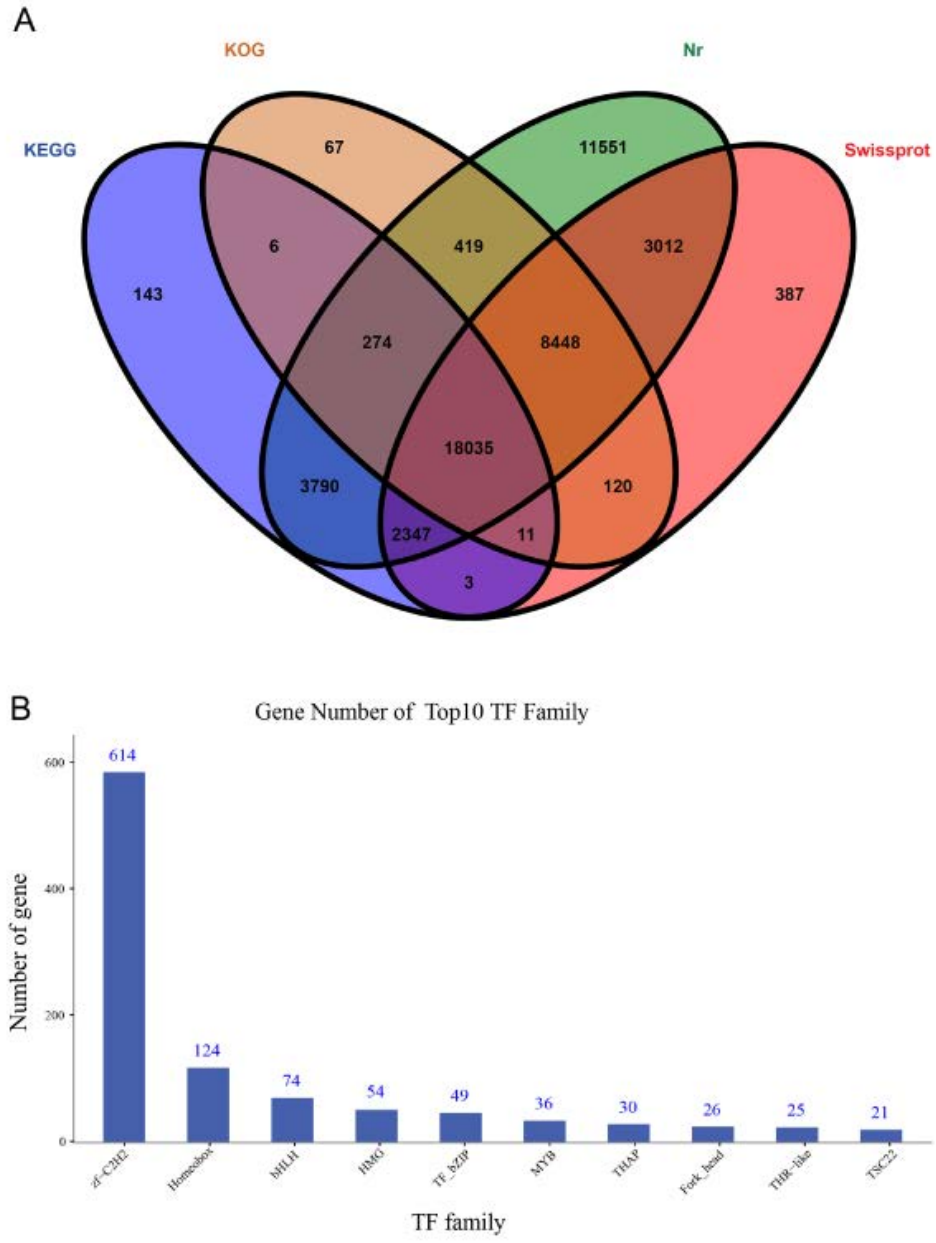

Fig S1. Annotation of unigenes.

(A) Venn diagram showing the basic annotation of the assembled unigenes. Sequence similarity searches against various protein database including non-redundant (nr) protein, SwissProt, Clusters of Orthologous Groups (COG/KOG) and Kyoto Encyclopedia of Genes and Genomes (KEGG) databases. (B) Transcription factors (TF) classification of the unigenes of amphioxus.

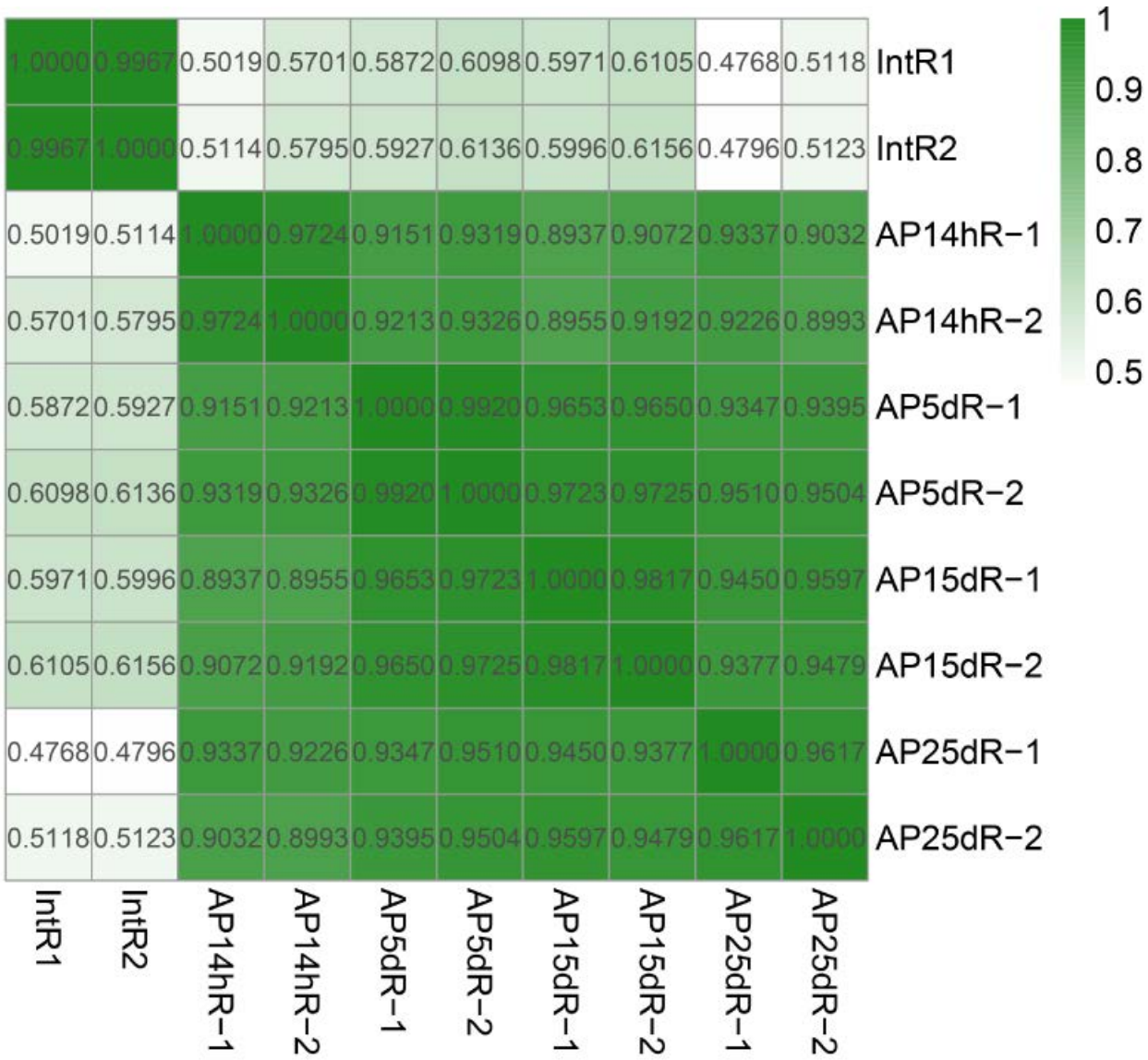

Fig S2. Heat map showing Pearson correlation between two samples.

Within a group, when the Pearson correlation between two samples is close to 1, it means that the two samples are highly related.

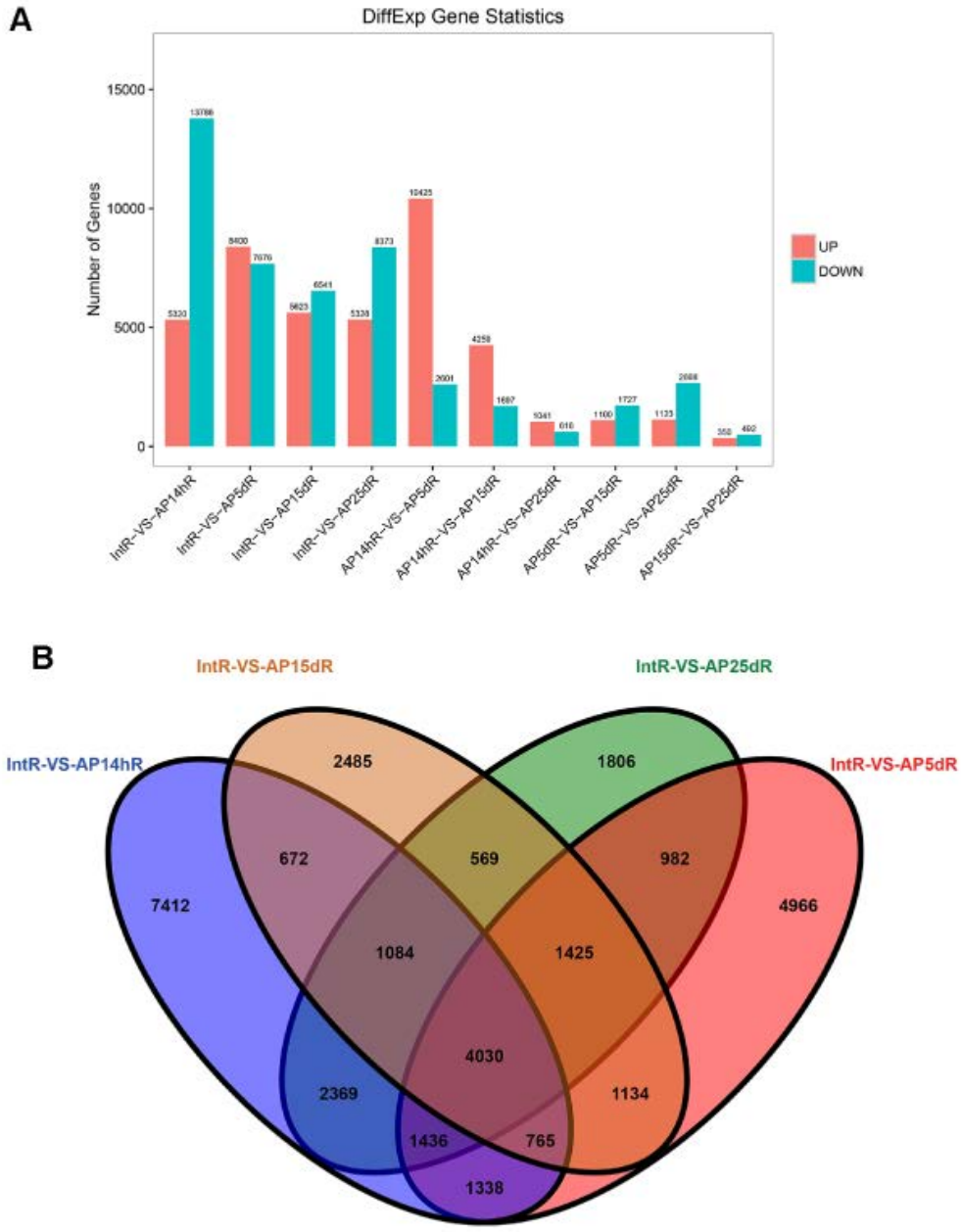

Fig S3. Statistics of differentially-expressed genes between different regeneration stages.

(A) Bar graph shows the up-regulated and down-regulated gene numbers between two different tissues. (B) Venn diagram shows DEGs shared by different regenerative stages respective to the intact tail. IntR means intact tail, and AP14hR, AP5dR, AP15dR and AP25dR mean tail regenerates at 14 h, 5 d, 15 d and 25 d post-amputation respectively.

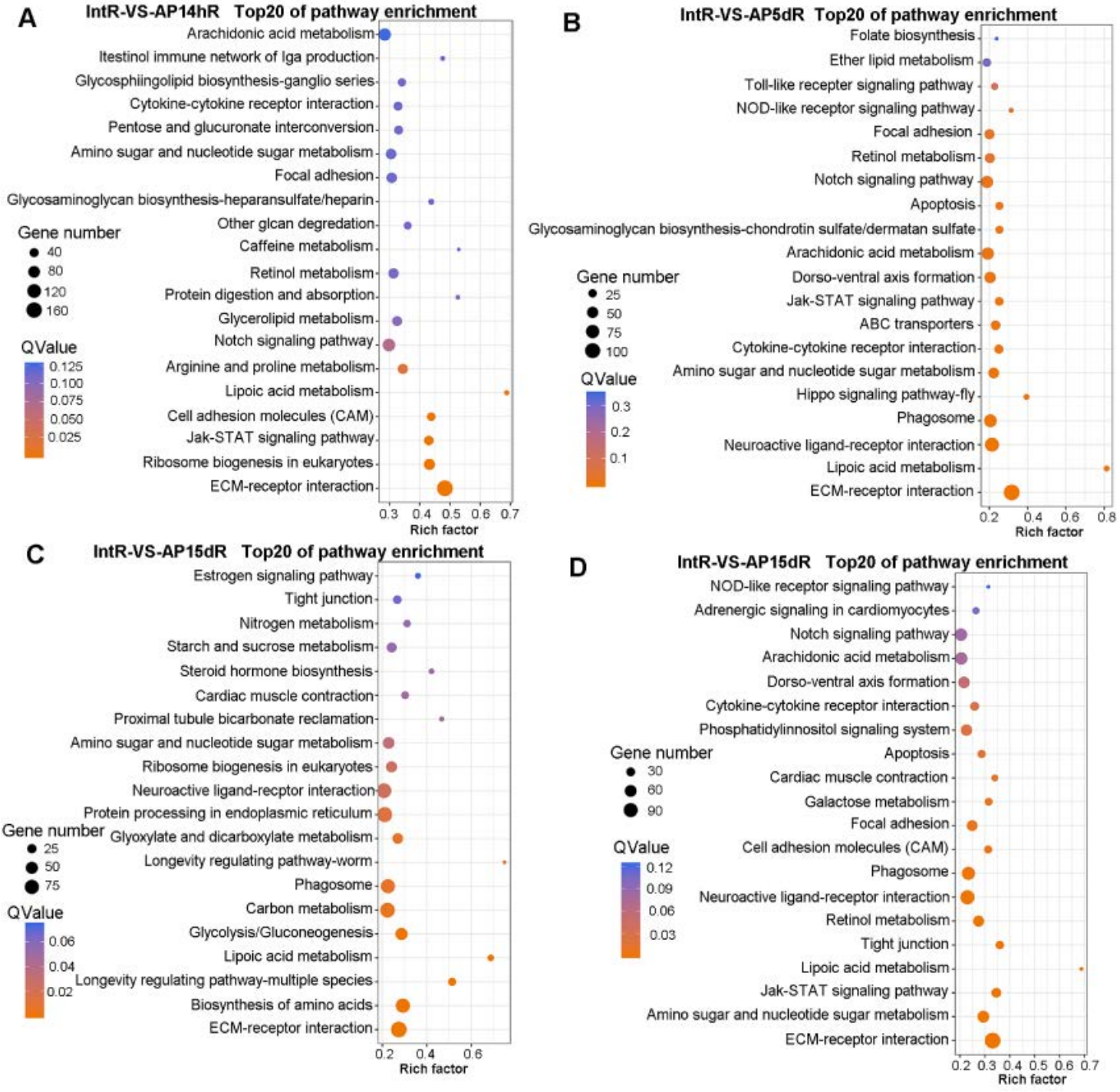

Fig S4. KEGG analysis of DEGs of tail regenerates at different regenerative stages, compared to intact tails.

(A) Top 20 pathways by enrichment of DEGs of tail regenerates at 14 h post-amputation. (B) Top 20 pathways by enrichment of DEGs of tail regenerates at 5 d post-amputation. (C) Top 20 pathways by enrichment of DEGs of tail regenerates at 15 days post-amputation. (D) Top 20 pathways by enrichment of DEGs of tail regenerates at 25 d post-amputation. Rich Factor is the ratio of differentially expressed gene numbers annotated in this pathway terms to all gene numbers annotated in this pathway term. Q value means corrected P value, $Q < 0.05$ as significantly enriched.

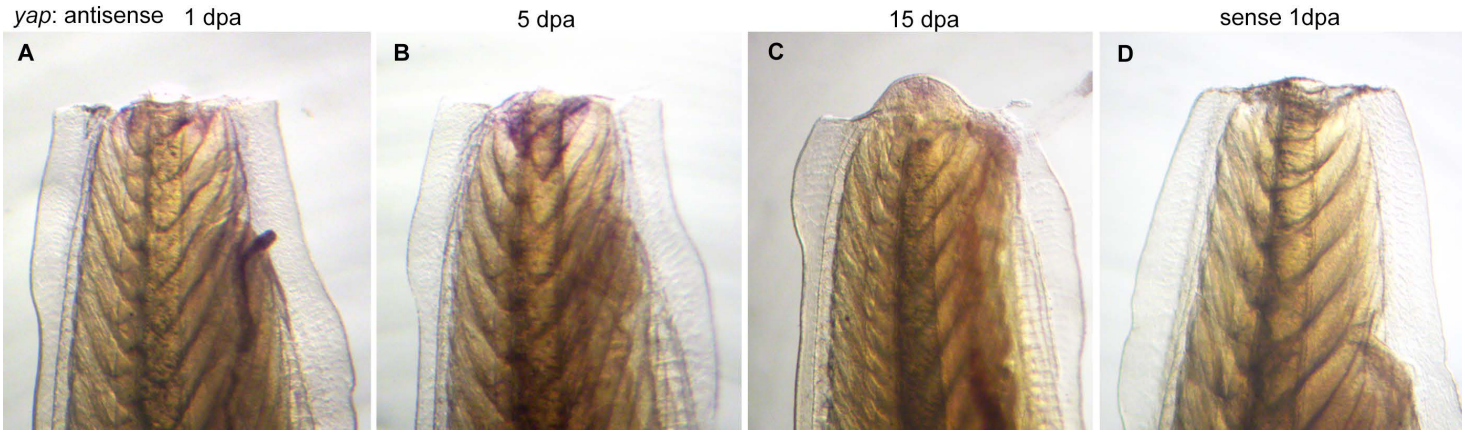

Fig S5. Whole-mount *in situ* hybridization analysis of *yap* expression during tail regeneration process.

(A-C) tail regenerates at 1 day, 5 days and 15 days post-amputation respectively, hybridized with antisense probes. (D) tail regenerate at 1 day post-amputation, hybridized with the sense probes. The blue represents positive staining for *yap* expression. All panels are tail regenerates with distal at the top.

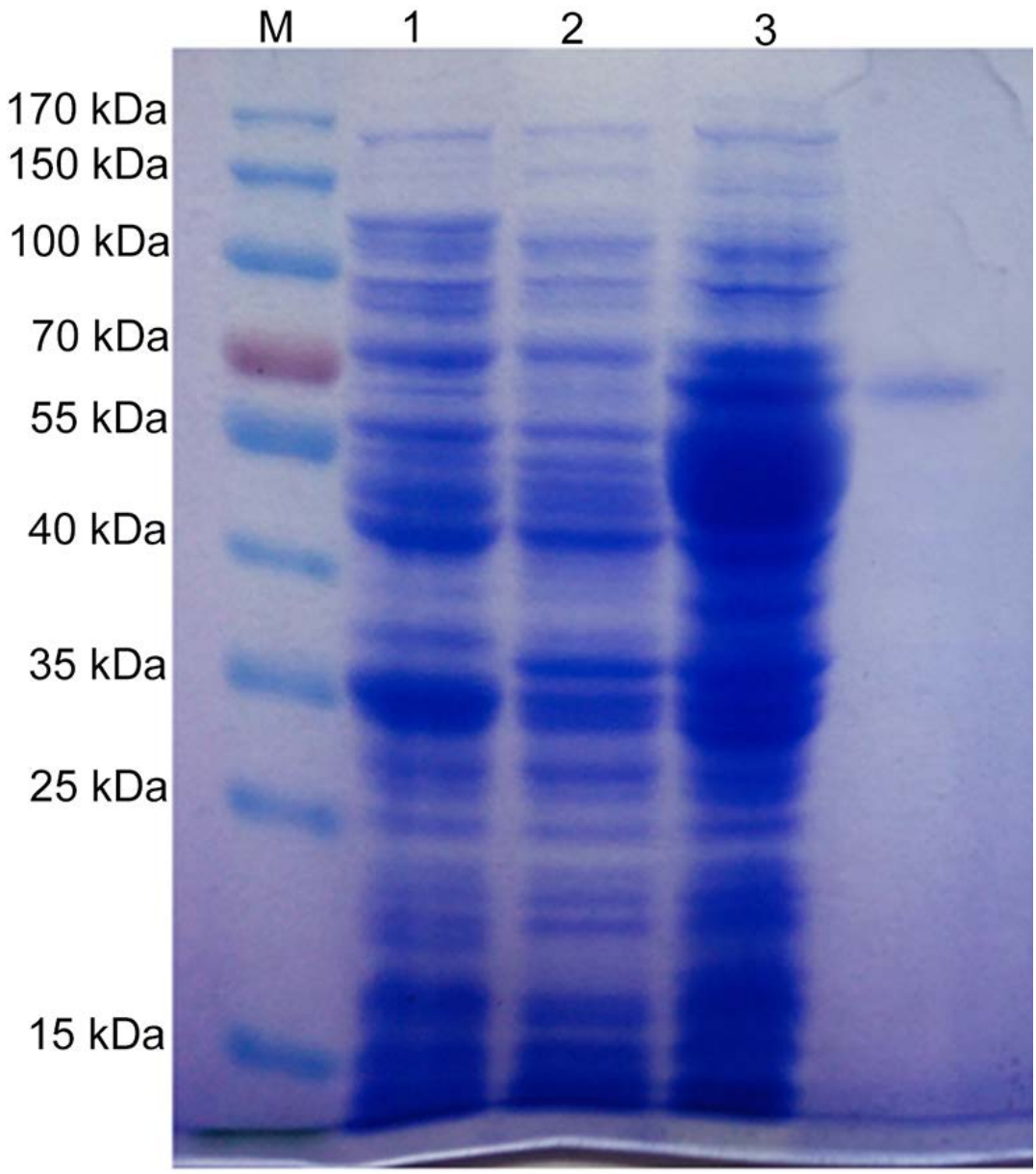

Fig S6. SDS-PAGE analysis of the expression and purification of recombinant BMP2/4 from *E. coli* cells.

Lane M, molecular mass standards; lane 1, extracts from *E. coli* BL21 containing pET32a empty vector; lane 2, extracts from *E. coli* BL21 containing pET32a/BMP2/4 before induction; lane 3, total cellular extracts from IPTG-induced E. coli BL21 containing pET32a/BMP2/4; lane 4, recombinant BMP2/4 purified on NiNTA resin column.

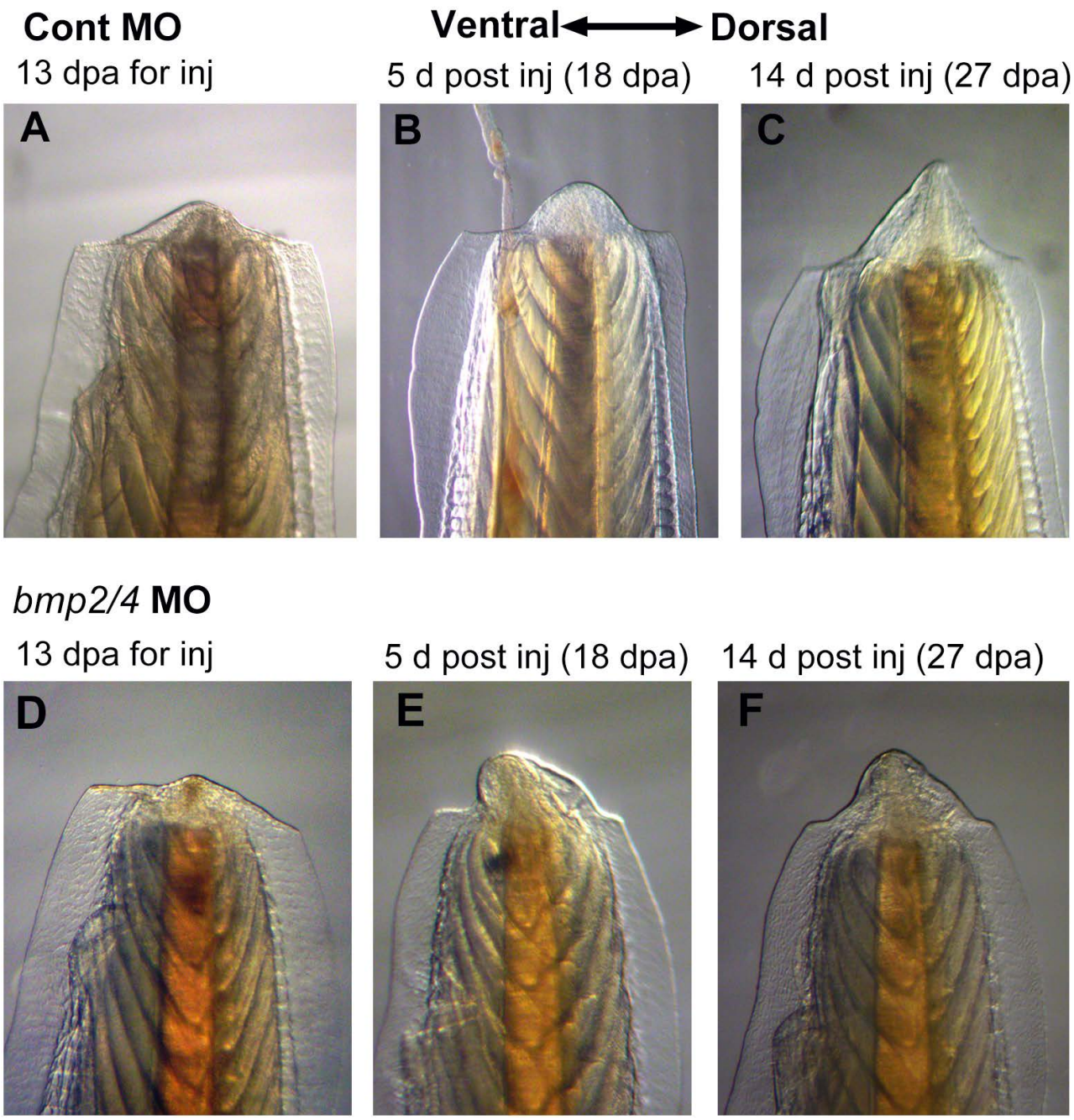

Fig. S7. vivo-morpholino mediated BMP2/4 knockdown disturbed the patterning of the regenerative blastema.

(A-C) tail regenerates at different time points post injection of control MO. (D-F) Tail regenerates at different time points post injection of BMP2/4 MO. The BMP2/4 MO caused the tail blastema to grow and fold toward ventral side of the body, compare to the controls. dpa means days post-amputation. d post inj means days post-injection.

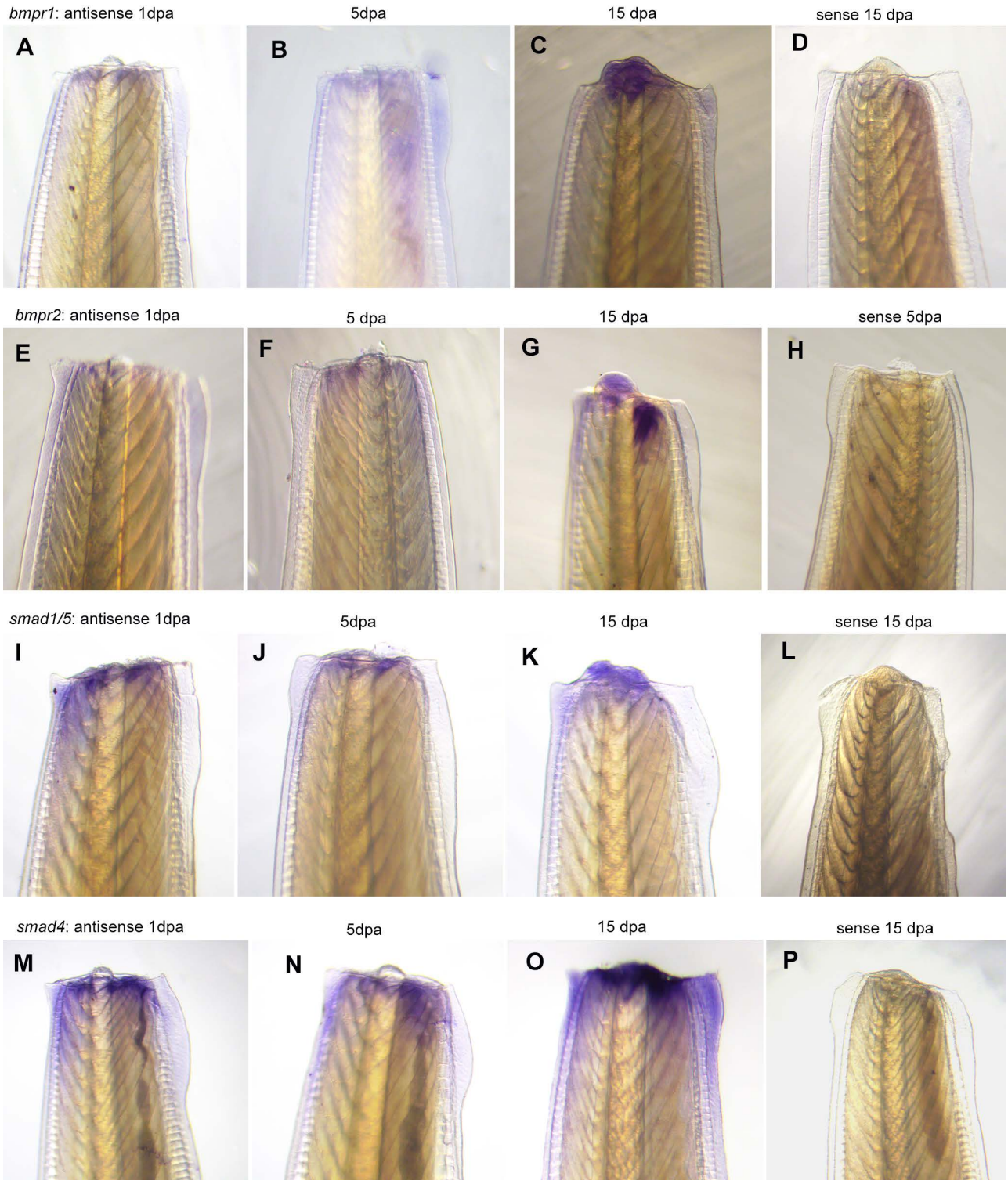

Fig. S8. Whole-mount *in situ* hybridization analysis of expression patterns of BMP signaling related genes during tail regeneration process.

(A-D) expression of *bmpr*1 during tail regeneration process. (E-H) expression of *bmpr*2 during tail regeneration process. (I-L) expression of *smad1/5* during tail regeneration process. (M-P) expression of *smad4* during tail regeneration process. All the four BMP signaling genes were specifically expressed in wound region at wound healing stage, and their expressions were also specially detected in the newly formed blastema at blastemal stage. (D, H, L and P) Controls for the genes respectively, and no positive staining signals were detected. dpa means days post-amputation.

Table S1. Assignment of Unigenes into TF families

Click here to download Table S1

Table S2. Description of DEGs at early wound healing stage (14 hpa), compared to intact tail.

Click here to download Table S2

Table S3. Description of DEGs at late wound healing stage (5 dpa), compared to intact tail.

Click here to download Table S3

Table S4. Description of DEGs at early blastema stage (15 dpa), compared to intact tail.

Click here to download Table S4

Table S5. Description of DEGs at late blastema stage (25 dpa), compared to intact tail.

Click here to download Table S5

Table S6. Biological processes classification in GO enrichment of up-regulated DEGs at early wound healing stage (14 hpa), compared to intact tail.

Click here to download Table S6

Table S7. Biological processes classification in GO enrichment of up-regulated DEGs at late wound healing stage (5 dpa), compared to intact tail.

Click here to download Table S7

Table S8. Description of the genes listed in Fig. 4A.

Click here to download Table S8

Table S9. Biological processes classification in GO enrichment of up-regulated DEGs at early blastemal stage (15 dpa), compared to intact tail.

Click here to download Table S9

Table S10. Biological processes classification in GO enrichment of up-regulated DEGs at late blastemal stage (25 dpa), compared to intact tail.

Click here to download Table S10

Table S11. Description of the genes listed in Fig. 4B.

Click here to download Table S11

Table S12. KEGG classification of up-regulated DEGs at early wound healing stage (14 hpa), compared to intact tail.

Click here to download Table S12

Table S13. KEGG classification of up-regulated DEGs at late wound healing stage (5 dpa), compared to intact tail.

Click here to download Table S13

Table S14. KEGG classification of up-regulated DEGs at early blastemal stage (15 dpa), compared to intact tail.

Click here to download Table S14

Table S15. KEGG classification of up-regulated DEGs at late blastemal stage (25 dpa), compared to intact tail.

Click here to download Table S15